43. M. A. Lauffer, *Entropy-Driven Processes* (Springer-Verlag, New York, 1975).
44. W. Saenger, *Principles of Nucleic Acid Structure* (Springer-Verlag, New York, 1986).
45. C. R. Cantor and P. R. Schimmel, *Biophysical Chemistry Part III* (Freeman, San Francisco, 1980), pp. 1109–1264.
46. P. R. Schimmel, *Annu. Rev. Biochem.* **56**, 125 (1987); A. A. Bogdanov, *Trends Biol. Sci.* **14**, 505 (1989); C. W. A. Pleij, *ibid.* **15**, 143 (1990).
47. E. J. Corey and X.-M. Ming, *The Logic of Chemical Synthesis* (Wiley, New York, 1989).
48. D. B. Smithrud, T. B. Wyman, F. Diederich, *J. Am. Chem. Soc.* **113**, 5420 (1991).
49. J. M. McCammon and S. G. Harvey, *Dynamics of Proteins and Nucleic Acids* (Cambridge Univ. Press, New York, 1987); W. L. Jorgenson, *CHEMTRACTS* **4**, 91 (1991).
50. M. C. Etter, *Acc. Chem. Res.* **23**, 120 (1990); J. A. Zerkowski, C. T. Seto, D. A. Wierda, G. M. Whitesides, *J. Am. Chem. Soc.* **112**, 9025 (1990); M. C. Etter, *J. Phys. Chem.* **95**, 4601 (1991).
51. R. W. Saalfrank, A. Stark, M. Bremer, H.-U. Hummel, *Angew. Chem. Int. Ed. Engl.* **29**, 311 (1990).
52. J.-M. Lehn, *ibid.* **27**, 89 (1988); C. J. Pedersen, *ibid.*, p. 1021 (1988); D. J. Cram, *ibid.*, p. 1009; F. Diederich, *ibid.*, p. 362; J. F. Stoddart, *Annu. Rep. Prog. Chem. Sect. B* **86**, 353 (1989).
53. H. W. Deckman *et al.*, *J. Vac. Sci. Technol. B* **6**, 333 (1988).
54. G. D. Stucky *et al.*, *J. Am. Chem. Soc.* **111**, 8006 (1989); G. A. Ozin *et al.*, *Adv. Mater.* **3**, 306 (1991).
55. J. Rebek, Jr., *Angew. Chem. Int. Ed. Engl.* **29**, 245 (1990).
56. C. A. Hunter and J. K. M. Sanders, *J. Am. Chem. Soc.* **112**, 5525 (1990).
57. The CA·M cyclic hexamer is the presumed structure of the 1:1 complex formed between cyanuric acid and melamine. The results from powder diffraction studies are consistent with this structural motif (J. Zerkowski, R. Graham, G. M. Whitesides, unpublished results). The crystal structure of the CA·M·3HCl complex has been reported [Y. Wang, B. Wei, Q. Wang, *J. Crystallogr. Spectrosc. Res.* **20**, 79 (1990)].
58. C. T. Seto and G. M. Whitesides, *J. Am. Chem. Soc.* **112**, 6409 (1990).
59. ———, *ibid.* **113**, 712 (1991).
60. J. S. Manka and D. S. Lawrence, *ibid.* **112**, 2440 (1990).
61. U. Koert, M. M. Harding, J.-M. Lehn, *Nature* **346**, 339 (1990).
62. D. Philp and J. F. Stoddart, *Synlett* (1991), p. 445.
63. G. Prakash and E. T. Kool, *J. Chem. Soc. Chem. Commun.* **1991**, 1161 (1991).
64. S. L. Tang, *Chem. Tech.* (1991), p. 182.
65. N. P. Pavletich and C. O. Pabo, *Science* **252**, 809 (1991).
66. R. Breslow, *ibid.* **218**, 532 (1982); see also *Carbohydr. Res.* **192**, 1-370 (1989) for a full overview of cyclodextrin research.
67. See (*26*), p. 218.
68. Supported in part by the National Science Foundation (grants no. CHE 88-12709 and no. DMR 89-20490) and by the Office of Navel Research and the Defense Advanced Projects Research Agency (grant no. N00014-86-K-0756). J.P.M. acknowledges support from the Science and Engineering Research Council in the United Kingdom for a NATO Postdoctoral Fellowship (1991–93).

Atomic and Molecular Manipulation with the Scanning Tunneling Microscope

JOSEPH A. STROSCIO AND D. M. EIGLER

The prospect of manipulating matter on the atomic scale has fascinated scientists for decades. This fascination may be motivated by scientific and technological opportunities, or from a curiosity about the consequences of being able to place atoms in a particular location. Advances in scanning tunneling microscopy have made this prospect a reality; single atoms can be placed at selected positions and structures can be built to a particular design atom-by-atom. Atoms and molecules may be manipulated in a variety of ways by using the interactions present in the tunnel junction of a scanning tunneling microscope. Some of these recent developments and some of the possible uses of atomic and molecular manipulation as a tool for science are discussed.

THE SCANNING TUNNELING MICROSCOPE (STM) CAN IMAGE the surface of conducting materials with atomic-scale detail. As with other microscopes, we use the STM to extend our vision to a realm where our eyes cannot see. In tunneling microscopy we conventionally record an image that is a map of the trajectory of a probe tip over a surface while the height of the probe tip is constantly adjusted to maintain a constant tunneling current between the tip and the surface. Such images reflect both the topography and the electronic structure of the surface (*1*). The STM may also be used to locally modify surfaces (*2*). In the last few years efforts along these lines have culminated in the ability to manipulate individual atoms and molecules with atomic-scale precision, a goal that has intrigued scientists for decades (*3*). In a sense, we may use the STM to extend our touch to a realm where our hands are simply too big. In this article we review how the STM may be used to manipulate matter on the atomic scale and discuss the physical mechanisms involved.

A variety of different atomic manipulation processes have been demonstrated with the STM. We may divide these processes into two classes: parallel processes and perpendicular processes. In parallel processes an adsorbed atom or molecule is induced to move along the surface. In perpendicular processes the atom or molecule is transferred from the surface to the tip of the STM or vice versa. In both processes the goal is the purposeful rearrangement of matter on the atomic scale. We may view the act of rearrangement as a series of steps that results in the selective making and breaking of chemical bonds between atoms, or, equivalently, as a procedure that causes a configuration of atoms to evolve along some time-dependent potential energy hypersurface from an initial to a final configuration. Both points of view should prove useful in understanding the physical mechanisms by which atoms may be manipulated with the STM.

Parallel Processes

The first class of atomic manipulation processes that we discuss is parallel processes, that is, processes in which the motion of the manipulated adsorbate atom or molecule is parallel to the surface. We discuss two parallel processes, field-assisted diffusion and the sliding process. In this class of processes the bond between the manipulated atom and the underlying surface is never broken, by

J. A. Stroscio is a physicist in the Electron and Optical Physics Division, National Institute of Standards and Technology, Gaithersburg, MD 20899. D. M. Eigler is a Research Staff Member of the IBM Research Division, Almaden Research Center, San Jose, CA 95120.

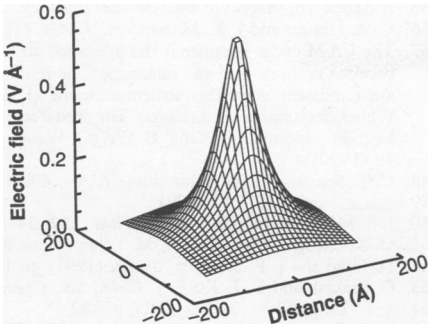

Fig. 1. Spatial dependence of the electric field in an STM tunnel junction calculated for a 100 Å radius tip positioned 5 Å above a planar metal surface with a 3-V potential difference. The tip is modeled as a 100 Å radius sphere 5 Å above a semi-infinite metal surface. The electric field is calculated at the position of the metal surface.

which we mean that the adsorbate always lies well within the adsorption well. The relevant energy scale for these processes is the energy of the barrier to diffusion across the surface (sometimes called the corrugation energy). This energy is typically in the range of 1/10 to 1/3 of the adsorption energy and thus varies from tens of millivolts for a weakly bound physisorbed atom on a close-packed metal surface, such as Xe on Pt(111), up to about 0.1 to 1.0 eV for a strongly bound chemisorbed atom.

Field-Assisted Diffusion

The presence of the intense electric field between the probe tip and the surface is usually overlooked in normal STM imaging. With a tunneling gap spacing of 5 Å and a potential difference of 1 to 10 V, the electric field strength is in the range of from 0.2 to 2 V $Å^{-1}$. This field is inhomogeneous and concentrated in the vicinity of the probe tip, as shown in Fig. 1 for a 100 Å radius tip positioned 5 Å above a metal surface with a 3-V potential difference. These large fields can be compared to the field strength required for field ionization and desorption of an atom (*4*), which is around 3 to 5 V $Å^{-1}$. Field-assisted manipulation of atoms is possible at lower fields, where the interaction of the spatially inhomogeneous electric field with the dipole moment of an adsorbed atom can lead to a potential energy gradient, or force along the surface, which results in a field-assisted directional diffusion of the adatom. Field-assisted directional diffusion is not only a manipulation technique but also offers the ability to measure the dipole moment and polarizabilities of adatoms, as has been demonstrated in field-ion microscopy (FIM) studies and field electron emission studies (*5*–*7*).

Electric field–assisted directional diffusion in the STM was demonstrated by Whitman *et al.* with Cs atoms on GaAs and InSb(110) surfaces (*8*). Previously, Stroscio and co-workers had shown that STM imaging of Cs atoms on these surfaces displays stable structures with the sample at negative polarity (−2 to −3 V), consisting of one-dimensional zigzag rows of Cs atoms at low Cs densities (see inset in Fig. 2) (*9, 10*). However, when the sample was held at positive polarity there was a substantial flux of Cs into the region of highest electric field below the apex of the tip (a tip radius of about 100 to 200 Å was determined from electron micrographs and FIM studies). This process is shown in Fig. 2: first an area is imaged at negative sample polarity; the voltage is then switched to positive polarity for short time intervals while the tip is stationed in the center of the imaged area; and finally the area is reimaged at negative polarity. As observed in Fig. 2, the Cs atoms are seen to have preferentially diffused toward the center of the image. The amount by which diffusion increased with the length of the voltage pulse is shown in Fig. 2, D to F. These data are more quantitatively shown in Fig. 3A, which displays the histograms of the difference in Cs chain length distributions after the voltage pulse. The Cs distributions shift to longer chain lengths as a function of pulse length, increasing the number of Cs atoms in the underlying area.

Directional diffusion can be discussed in terms of the potential energy gradient of an atom in an electric field (*5*–*7*), although a number of unresolved issues remain to be explored (*8*). An atom in an electric field becomes polarized with a dipole moment given to first order in E as

$$\mathbf{p} \simeq \boldsymbol{\mu} + \vec{\boldsymbol{\alpha}}\mathbf{E} + \ldots \quad (1)$$

where $\boldsymbol{\mu}$ is the static dipole moment, $\vec{\boldsymbol{\alpha}}\mathbf{E}$ is the induced dipole moment, and $\vec{\boldsymbol{\alpha}}$ is the polarizability tensor. The spatially dependent energy of the atom would then be given by

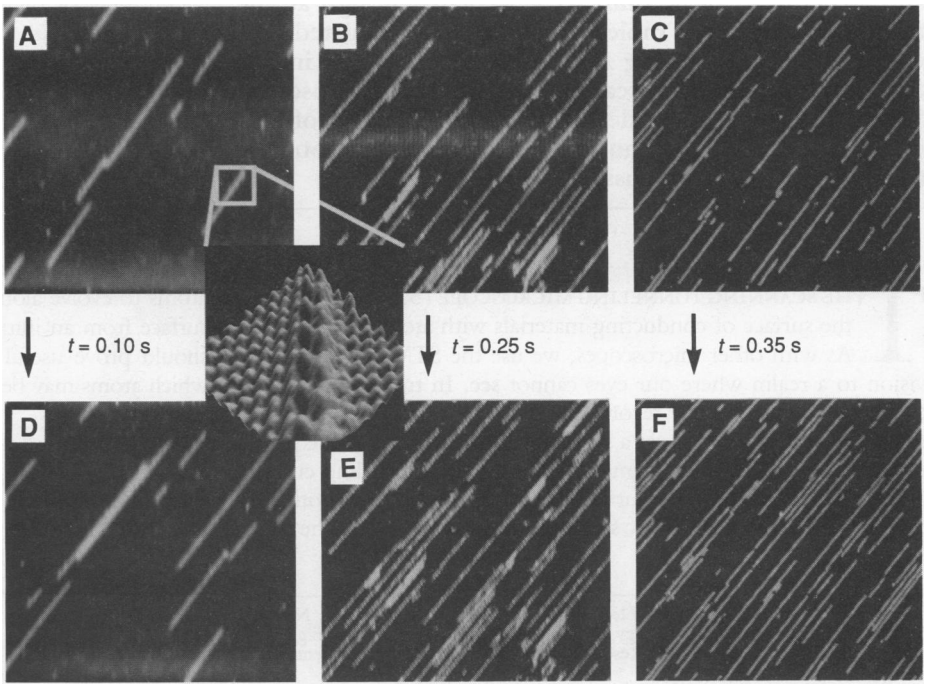

Fig. 2. STM images of Cs on *p*-type GaAs(110) surfaces. (**A** through **C**) Images recorded at −2-V sample bias showing the initial state before pulsing the voltage. The inset in (A) shows an atomic resolution 70 Å by 70 Å image of the Cs zigzag structure on GaAs(110). (**D** through **F**) Images recorded at −2.5 V after pulsing the sample voltage to +1 V, with the tip positioned in the center of the image for 0.15, 0.25, and 0.35 s, respectively. All of the images are 1400 Å by 1400 Å, except (A) and (D), which are 1000 Å by 1000 Å.

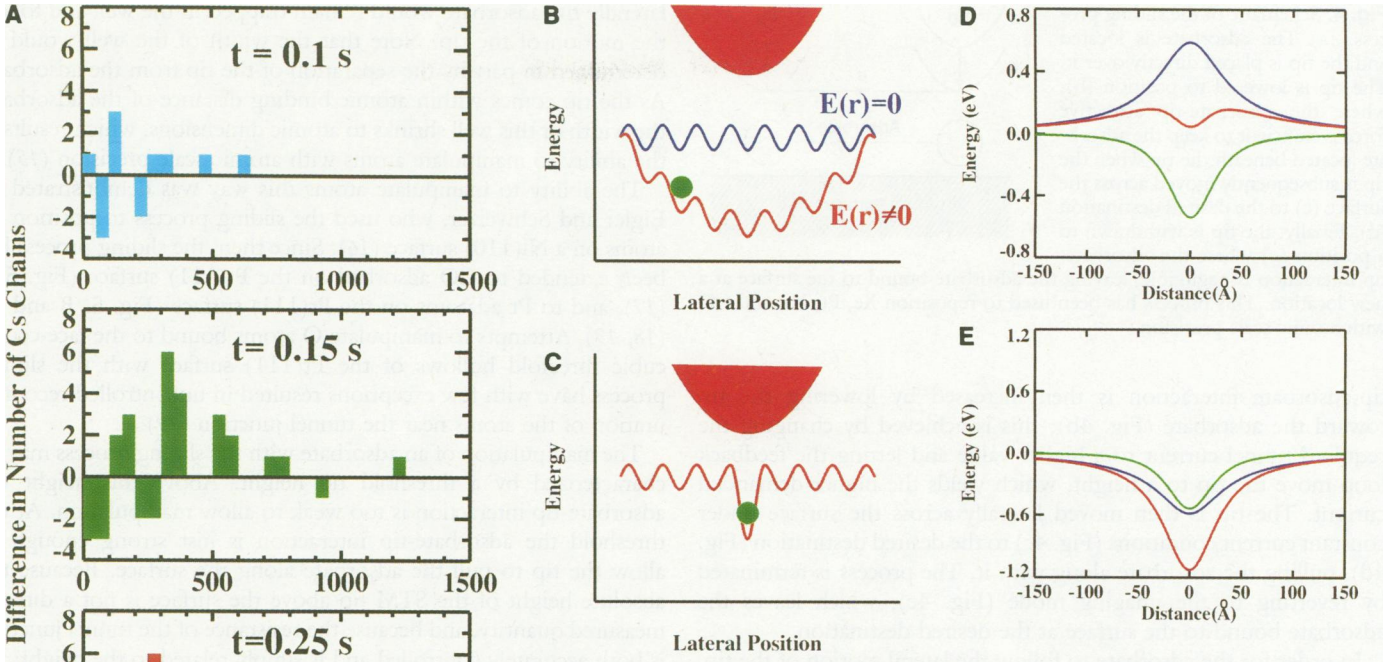

Fig. 3. (**A**) Histograms of the Cs chain lengths obtained from subtracting the Cs distributions before pulsing the field from the distributions obtained after applying a +1-V pulse to the sample for the indicated pulse lengths. (**B** and **C**) Schematic of the potential energy of an adsorbate as a function of its lateral position on a surface above which there is located the STM tip (shown in red). Interaction with the atoms of the underlying surface gives rise to the weak periodic corrugation of the energy. (B) The interaction of the electric field with the adsorbate dipole moment gives rise to a broad potential well where an atom, shown in green, would feel a force to move it to the bottom of the well under the apex of the tip. (C) An attraction of an adsorbate to the tip by a chemical binding force gives rise to a potential well located directly below the tip. If the side walls of this well can be made steep enough, then the adsorbate (shown in green) would remain trapped in the well as the tip is moved laterally. (**D** and **E**) Potential energy from Eq. 2 derived from the field profile shown in Fig. 1 for (D) −3-V and (E) +3-V sample bias. A dipole moment of 1.6×10^{-27} C cm and a polarizability of 50 Å^3 was used. The two terms contributing to the potential energy are shown, the static-dipole term in blue and the induced-dipole term in green. The sum of the two terms is shown in red.

$$U(\mathbf{r}) = -\boldsymbol{\mu}\cdot\mathbf{E}(\mathbf{r}) - \frac{1}{2}\vec{\boldsymbol{\alpha}}\mathbf{E}(\mathbf{r})\cdot\mathbf{E}(\mathbf{r}) + \ldots \quad (2)$$

This potential energy is added to the periodic surface potential (Fig. 3B).

The potential energy gradient (Fig. 3B) would cause the adatoms to diffuse toward the potential minimum under the tip. Diffusion is a statistical process that depends on the attempt frequency and the potential barriers. Directional diffusion of atoms in strong electric fields is well known from FIM studies (*5*–*7*). Observing diffusion with the STM shows a number of differences with respect to these previous FIM studies. The most noticeable is the absence of diffusion at negative sample polarity (Fig. 2). This difference implies an induced dipole of similar magnitude and opposite sign as the static dipole term, yielding a net dipole moment near zero (see Eq. 1) at a field strength of about -0.4 V Å^{-1}.

The potential energy modification estimated for an adsorbed Cs atom with a tip-sample potential difference of 3 and −3 V is shown in Fig. 3, D and E. The dipole moment $\mu = 1.6 \times 10^{-27}$ C cm was estimated from work function measurements (*11*), and the polarizability α = 50 Å^3 (5×10^{-35} C cm^2 V^{-1}) was taken to yield a nearly zero dipole moment at −3 V (see Fig. 3D). In Fig. 3E we see that the static and induced dipole terms in the potential energy are of the same sign and similar magnitude for a +3-V sample bias. These terms add to give a potential lowering of ~1 eV in the region of highest field (Fig. 3E). This value can be compared to the diffusion barriers of alkali atoms on GaAs(110); calculated values give a barrier of ~0.1 eV along the [1$\bar{1}$0] GaAs rows and ~1.0 eV perpendicular to the GaAs rows, that is, the [001] direction (*12*).

At negative sample polarity the static and induced dipole terms cancel to give an absence of a significant potential well for diffusion (Fig. 3D), which implies a value of the polarizability $\alpha \approx 50$ Å^3. Although this value seems reasonable for gas-phase alkali atoms, it is about ten times larger than observed in diffusion studies of Cs on metal surfaces (*7*). The polarizability of the alkali metal atoms may be enhanced in this case since they are adsorbed on a semiconductor rather than metal surface. Recent quantum cluster calculations for Cs on GaAs(110) show an enhanced polarizability on the order of 50 Å^3, which is close to the value deduced above (*13*).

Sliding Process

The tip of an STM always exerts a force on an adsorbate bound to the surface. One component of this force is due to the interatomic potential, that is, the chemical binding force, between the adsorbate and the outermost tip atom or atoms. By adjusting the position of the tip we may tune the magnitude and the direction of the force exerted on the adsorbate by the tip. Hence, we have the potential to manipulate the adsorbate by pulling it across the surface with the tip; we call this the sliding process (*14*).

The sliding process consists of the steps depicted in Fig. 4. The adsorbate to be moved is first located with the STM in its imaging mode and then the tip is placed near the adsorbate (Fig. 4a). The

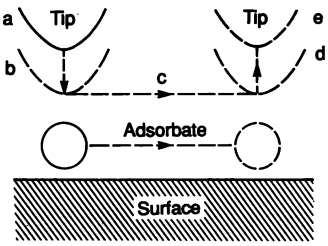

Fig. 4. Schematic of the sliding process. (a) The adsorbate is located and the tip is placed directly over it. The tip is lowered to position (b), where the adsorbate-tip attractive force is sufficient to keep the adsorbate located beneath the tip when the tip is subsequently moved across the surface (c) to the desired destination (d). Finally, the tip is withdrawn to a position (e) where the adsorbate-tip interaction is negligible, leaving the adsorbate bound to the surface at a new location. This process has been used to reposition Xe, Pt, Ni, and CO with atomic-scale precision.

tip-adsorbate interaction is then increased by lowering the tip toward the adsorbate (Fig. 4b); this is achieved by changing the required tunnel current to a higher value and letting the feedback loop move the tip to a height, which yields the higher demanded current. The tip is then moved laterally across the surface under constant current conditions (Fig. 4c) to the desired destination (Fig. 4d), pulling the adsorbate along with it. The process is terminated by reverting to the imaging mode (Fig. 4e), which leaves the adsorbate bound to the surface at the desired destination.

In order for the adsorbate to follow the lateral motion of the tip, the tip must exert enough force on the adsorbate to overcome the lateral forces between the adsorbate and the surface. Roughly speaking, the force necessary to move an adsorbate from site to site across a surface is given by the ratio of the corrugation energy to the separation between atoms of the underlying surface. However, the presence of the tip may also cause the adsorbate to be displaced normal to the surface relative to its unperturbed position. The displaced adsorbate would have an altered in-plane interaction with the underlying surface. If the tip pulls the adsorbate away from the surface causing a reduction of this in-plane interaction, then we would expect our estimate to be an upper bound for the force necessary to move the adsorbate across the surface.

One way to view the sliding process is that the position of the adsorbate evolves along a locally minimum energy trajectory on a time-dependent energy hypersurface. A schematic depiction of one cut through the energy hypersurface (Fig. 3C) shows the energy of the adsorbate as a function of its lateral position on the surface and in the presence of the tip. The interaction of the adsorbate with the surface gives rise to the corrugated potential. The lateral interaction with the tip results in the energy well located just below the tip. If the walls of this well are steep enough and the temperature is so low that thermal diffusion is negligible, then when the tip is moved laterally the adsorbate would remain trapped in the well and follow the motion of the tip. Note that the width of the well would be determined in part by the separation of the tip from the adsorbate. As the tip comes within atomic binding distance of the adsorbate, the width of this well shrinks to atomic dimensions, which results in the ability to manipulate atoms with atomic-scale precision (*15*).

The ability to manipulate atoms this way was demonstrated by Eigler and Schweizer, who used the sliding process to position Xe atoms on a Ni(110) surface (*16*). Since then, the sliding process has been extended to CO adsorbed on the Pt(111) surface (Fig. 5A) (*17*), and to Pt adatoms on the Pt(111) surface (Fig. 5, B and C) (*18, 19*). Attempts to manipulate O atoms bound to the face-center cubic threefold hollows of the Pt(111) surface with the sliding process have with few exceptions resulted in uncontrolled reconfiguration of the atoms near the tunnel junction (*19*).

The manipulation of an adsorbate with the sliding process may be characterized by a threshold tip height. Above this height the adsorbate-tip interaction is too weak to allow manipulation. At the threshold the adsorbate-tip interaction is just strong enough to allow the tip to pull the adsorbate along the surface. Because the absolute height of the STM tip above the surface is not a directly measured quantity, and because the resistance of the tunnel junction is both accurately controlled and is simply related to the height, we characterize the height of the tip according to the resistance of the tunnel junction (increasing resistance corresponds to greater tip-sample separations, and hence to a weaker tip-sample interaction). The threshold resistance to slide an adsorbate depends on the particular arrangement of atoms at the apex of the tip, but not by more than a factor of 4. We find a threshold resistance of 5 MΩ for sliding Xe along the rows of the Ni(110) surface (*20*), a threshold of 200 kΩ for sliding CO along the Pt(111) surface (*19*), and a threshold of 20 kΩ for moving Pt adatoms across the Pt(111) surface (*19*). The ordering of these threshold resistances is consistent with the simple notion that the corrugation energy scales with the binding energy and thus greater force must be applied to move adsorbates that are more strongly bound to the surface.

Perpendicular Processes

The STM allows a second class of atomic manipulations that we call perpendicular processes, in which an atom, molecule, or group of atoms is transferred from the surface to the tip, or from the tip to the surface. For simplicity we discuss the case of transferring an adsorbate from the surface to the tip. The relevant energy for such

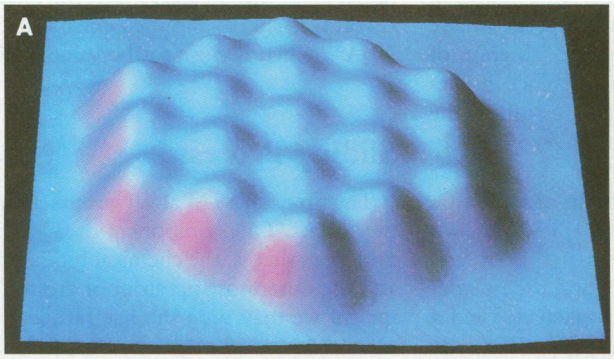

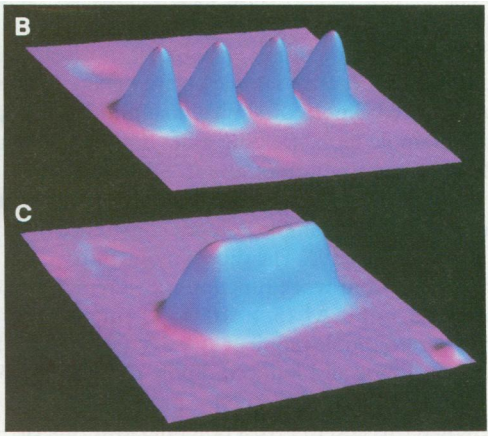

Fig. 5. (**A**) An island of CO molecules assembled in a $(\sqrt{3} \times \sqrt{3})$ R30° lattice on the Pt(111) surface by the sliding process. The image is 30 Å by 30 Å. (**B**) A 60 Å by 48 Å STM image of four Pt adatoms assembled into a linear array on the Pt(111) surface. The Pt adatoms appear as 1.43 Å high protrusions in this 10-nA constant-current image taken with the tip biased at −0.1 V. The Pt adatoms, which were originally located at random positions on the surface, were spaced four unit cells apart from each other along a close-packed direction of the Pt(111) surface. (**C**) A 40 Å by 40 Å STM image of a compact array of seven Pt adatoms on the Pt(111) surface demonstrating that the sliding process may be used to assemble close-packed structures of metal atoms. The vertical scales in all of these images are greatly expanded.

processes is the height of the energy barrier that the adsorbate must traverse in order to go from the surface to the tip. The height of this barrier depends on the separation of the tip from the surface; it approaches the adsorption energy in the limit of large tip-surface separation and goes to zero when the tip is brought close enough to the adsorbate. By adjusting the height of the tip we may tune the magnitude of this barrier to suit our purposes.

Transfer On- or Near-Contact

The transfer-on-contact process is conceptually the simplest of the atomic manipulation processes. In this process the tip is moved toward the adsorbate until the adsorption wells on the tip and surface sides of the junction coalesce, that is, the energy barrier separating the two wells is gone and the adsorbate can be considered simultaneously bound to the tip and the surface. The tip is then withdrawn, carrying the adsorbate with it. For the process to be successful the adsorbate's bond to the surface must be broken when the tip is withdrawn. We might expect that the adsorbate would "choose" to remain bound to the side of the junction on which it has the greatest binding energy. However, the "moment of choice" comes when the adsorbate has strong interactions with both tip and surface, so the binding energy argument may be too simple; it does not account for the simultaneous interaction of the adsorbate with the tip and the surface.

We have found that individual Xe adatoms may be reliably transferred from the terrace of a Pt(111) or a Ni(110) surface to most tips by the transfer-on-contact process (*21*). For Xe we see essentially no dependence of this process on the applied potential within the range ±0.05 V. We have also used this process to transfer Pt adatoms from a tip to a Pt(111) surface, but not with the degree of reliability observed for Xe. We infer that, in the case of Pt adatoms, the "choice" between binding to the surface or the tip is a sensitive function of the atomic arrangement of the tip atoms. We have also transferred entire benzene molecules to the tip this way and have returned them intact to the surface.

At a slightly increased separation between tip and sample, the adsorption wells of the tip and surface atom are close enough to significantly reduce the intermediate barrier but have it still remain finite, such that thermal activation is sufficient for atom transfer. We call this transfer-near-contact. This process has a rate proportional to $\nu \exp(-Q/kT)$, where ν is the frequency factor, Q is the reduced barrier between the tip and sample, k is Boltzmann's constant, and T is the absolute temperature. A transfer rate of 1 s^{-1} is obtained with a barrier reduced to ~0.75 eV, with $\nu \approx 10^{13}$ s^{-1} and $T = 300$ K. The transfer rate exhibits an anisotropy if the depth of the adsorption well is not the same on each side of the barrier. It is important to distinguish this transfer-near-contact mechanism from field evaporation, which requires an intermediate ionic state.

In its simplest form, the transfer-on(near)-contact process occurs in the complete absence of any electric field, potential difference, or flow of current between the tip and the sample. We anticipate that in some circumstances it should be possible to set the direction of transfer by biasing the junction during contact.

Field Evaporation

The idea that an atom could be transferred between the tip and surface due to the application of a voltage pulse was discussed by Gomer, who considered the conditions under which field evaporation of both positive and negative ions would occur (*22*). Field evaporation is described as a thermally activated evaporation of ions over the "Schottky" barrier formed by the lowering of the potential energy outside the conductor by the application of an electric field. A recent evaluation of the field evaporation process in STM geometry has been given by Tsong (*23*).

The first experimental indication that an atom might be purposefully transferred between the tip and surface of the STM is due to Becker *et al.*, who suggested that the atomic-scale perturbation left on a Ge surface was a Ge atom that had been transferred from a Ge "charged" tip to the surface by raising the bias of the tip to −4 V (*24*).

Further evidence for field-induced motion of atoms between tip and surface came from Mamin *et al.*, who demonstrated the ability to create ordered arrays of mounds on a surface (*25*). Mounds were formed by the application of 600-ns pulses of +3.6 V applied to an Au surface in an STM with an Au probe tip operated in air at room temperature. The formation of these mounds was found to take place only above a threshold electric field. Equivalent mounds could be formed at or above the same threshold electric field with reversed-polarity voltage pulses. Mamin *et al.* have argued that the mounds are formed of tip material that has been transferred to the surface by field evaporation of either positive or negative ions depending on the sign of the applied field. The tips showed no apparent degradation in their ability to create mounds even after having done so several thousand times. Nearly identical shaped mounds were created by Abraham *et al.* (*26*) by bringing a W tip into contact with an Au surface in a room-temperature ultrahigh vacuum (UHV) STM.

The first clear indication that individual atoms could be selectively removed from a surface by application of a voltage pulse came early in 1991 when a team of Hitachi scientists demonstrated the ability to remove individual S atoms from a MoS_2 surface at room temperature by bringing the tip to within 3 Å of the surface and applying a voltage pulse (*27, 28*). It was reported (*28*) that the Hitachi researchers believed that the atoms were removed by the field-evaporation mechanism.

More recently, Lyo and Avouris demonstrated that Si atoms could be reversibly transferred between a Si surface and a W probe tip of an STM in UHV at room temperature (*29*). In this work the application of a +3-V pulse to the Si surface results in a raised mound with a surrounding moat. The Si atoms could be pulled up under the apex of the tip, which is the point of highest field (see Fig. 1). The surrounding moat results from the removed Si atoms. Lyo and Avouris also showed that the Si mound could be picked up and moved with the application of additional voltage pulses. They attributed this to the field-evaporation mechanism.

A major difference observed in the STM process of field evaporation, compared to FIM studies, is the observation of a lower threshold for field evaporation. For example, in FIM studies, evaporation of Au and Si is observed in the range from 3 to 5 V $Å^{-1}$, compared to thresholds of 0.4 to 1.0 V $Å^{-1}$ in the STM work. A major difference in the STM geometry compared to FIM is the addition of a second electrode that needs to be taken into account. Tsong recently analyzed these differences and has concluded that the threshold field for ionization and evaporation would decrease by one half that appropriate for FIM only at tip-sample separations less than 4 Å. Field evaporation of negative ions, which has never been observed in FIM, is also considered unlikely in the STM geometry due to the competing effect of field electron emission, which would melt the tip or surface at the fields necessary for negative ion formation (*23*). This result brings into question whether field evaporation is the mechanism of atom transfer observed in the above works. Tsong (*23*) argues that a more likely explanation for the experiments by Mamin *et al.* is the melting and subsequent contact of the Au tip to produce the

mounds. At very close tip-sample separation, such as in the experiments by Lyo and Avouris (*29*), the distinction between transfer-near-contact (discussed above) and field evaporation becomes blurred and will require additional analysis to be understood.

Electromigration

The flow of electrical current can induce the migration of impurities or other defects through the bulk of a solid. This process is called electromigration. In a simple picture of electromigration (*30*) the force on the defect is thought to have two components. The first is due to a direct interaction of the effective charge on the defect with the electric field that drives the current. The second, which is called the "wind force," is due to the scattering of electrons at the defect. In an STM these forces should be most strongly felt by the atoms in the immediate vicinity of the tunnel junction where the electric field and current density are greatest. Ralls *et al.* (*31*) have suggested that an atom might be induced to move between the tip and the surface of an STM due the electromigration process.

Eigler *et al.* (*21*) have recently demonstrated the ability to reversibly transfer Xe atoms between a Ni(110) surface and the tip of an STM (both at 4 K) by application of voltage pulses. The Xe atom always moved in the same direction as the tunneling electrons. In contrast to the work of Mamin *et al.*, no threshold electric field was observed. Instead, for a particular applied voltage and tip-surface separation there existed some probability per unit time that the Xe atom would transfer between tip and surface. In addition, for a particular tip-surface separation corresponding to a resistance of 906 kΩ, they found that the rate $1/\tau$ at which the Xe atom transfers to the tip depends on the current I according to the power law $\tau^{-1} = I^{4.9\pm0.2}$. Such a power law dependence is consistent with the heating-assisted electromigration model proposed by Ralls *et al.* (*31*). In this model the defect is heated above the temperature of the lattice due to inelastic scattering of electrons at the defect. The vibrationally hot defect may then more easily hop to a neighboring site. The probability of finding an atom in a high-lying vibrationally excited state can have a power-law dependence on the current with an exponent greater than unity if multiple scattering events are required to promote the atom up the ladder of vibrational energy states. Further work is needed to conclusively demonstrate that electromigration drives the motion of the Xe atom.

A Tool for Science

The manipulation of matter on an atomic scale is a technical ability that we may now begin to exploit as a tool of scientific inquiry. We discuss below some of the ways in which atomic manipulation with the STM has already been used to this end. In addition, we point out future research directions that appear to be the most exciting and rewarding uses of this new tool.

Perhaps the most mundane but also most useful application of atomic manipulation is to modify STM tips so that they yield high-resolution images of surfaces. As an example, transferring a Xe atom to the tip (thus making the Xe atom the outermost tip atom) usually results in a tip that yields very high resolution images of the surface (*21*). Preparing a tip by transferring to it a known atom also provides an in situ technique for creating a tip about which the chemical identity of the outermost atom can be known.

One of the first uses of the sliding process was to "hand make" a linear chain of Xe atoms on a Ni(110) surface (Fig. 6A) (*16*). Besides demonstrating that such structures can be built, we also learn about the Xe-Ni system. First we learn that this particular structure is stable. Next we observe that the apparent spacing between the Xe atoms is 5.0 ± 0.2 Å, which corresponds to just twice the length of a unit cell of the underlying Ni(110) surface. We deduce that such linear chains of Xe atoms order commensurately with the underlying Ni lattice. This result indicates that the in-plane Xe-Ni interaction dominates over the in-plane Xe-Xe interaction. In solid Xe and in compact two-dimensional (2-D) islands of Xe on Pt(111), the Xe-Xe spacing is 4.4 Å. Accordingly, attempts to make a more compact linear array of Xe atoms along the rows of Ni atoms failed. In order to pull a Xe atom off the end of the chain, the tip had to be lowered closer to the atom than what was found to be necessary to move a lone Xe atom. Thus we learn that the Xe-Xe interaction along the chain is attractive. Similarly, the tip must be brought closer to the Xe atom in order to slide the atom perpendicular to the close-packed rows of atoms of the Ni(110) surface compared to sliding the atom parallel to the rows. The tip must be brought closer still to slide the Xe atom diagonally across the rows. These observations reflect the variation in the corrugation of the potential according to different directions along the surface.

Creating or synthesizing "custom" made structures is perhaps one of the most exciting applications of manipulation. It should be possible to create phases of matter that are not normally accessible in the laboratory. After creating these new structures, they can be investigated with the STM in the normal imaging and spectroscopic modes. The field-assisted diffusion method was used to show that a

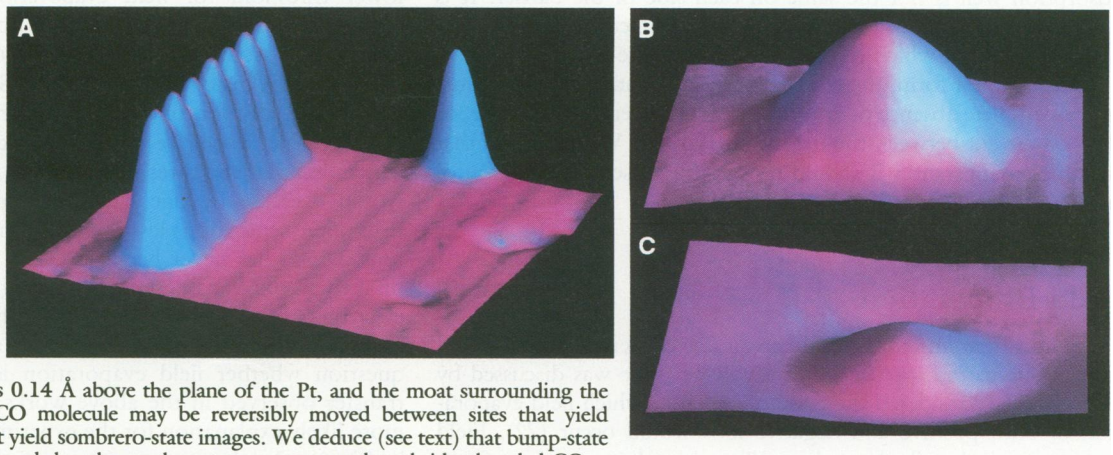

Fig. 6. (**A**) The first "hand-built" atomic structure. Seven Xe atoms bonded together to form a linear chain on the Ni(110) surface. The image is 50 Å by 50 Å. (**B** and **C**) Two 10 Å by 10 Å sequential STM images of a CO molecule on Pt(111) taken with the tip biased at −0.01 V and 1.0 nA of current. (B) "Bump"-state CO. The CO molecule appears as a 0.44 Å high cylindrically symmetric bump. (C) "Sombrero"-state CO. The peak of the sombrero protrudes 0.14 Å above the plane of the Pt, and the moat surrounding the peak is ~0.07 Å deep. The CO molecule may be reversibly moved between sites that yield bump-state images and sites that yield sombrero-state images. We deduce (see text) that bump-state CO is bound to the on-top site and that the sombrero state corresponds to bridge-bonded CO.

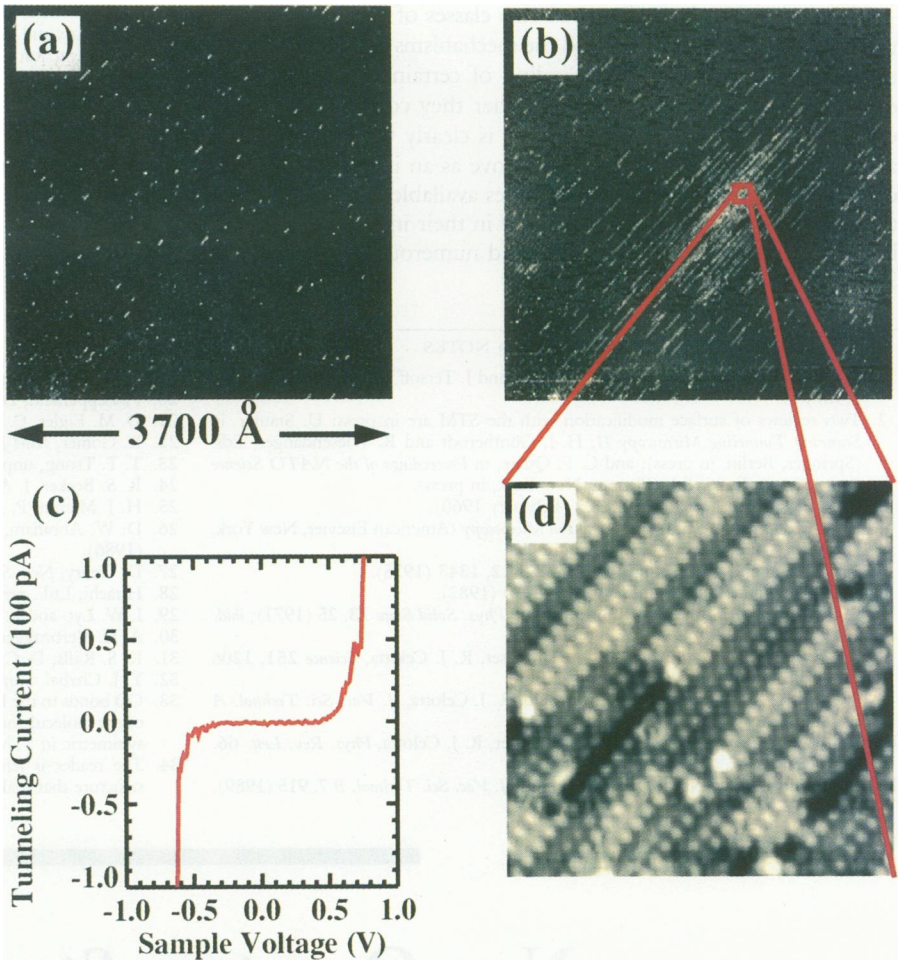

Fig. 7. STM images, 3500 Å by 3500 Å, of Cs on *p*-type GaAs(110) recorded (**A**) before and (**B**) after pulsing the sample bias to +3 V for 0.1 s with the tip at the center of the imaged area. (**C**) Current versus voltage measurement on the Cs phase in (D) showing nonmetallic characteristics with a band gap of 0.6 eV; (**D**) 200 Å by 200 Å image of the center region after pulsing the sample bias to +3 V for 0.1 s. The image consists of a close-packed 2-D phase of Cs on GaAs(110) formed by the voltage pulse that does not occur naturally.

new 2-D phase of Cs could be assembled on the GaAs(110) surface (Fig. 7D) (*8*). This structure is significant, since it does not occur following deposition of Cs, but is instead created from the lateral forces acting to close pack the Cs atoms together under the action of the pulsed electric field. One advantage of using the STM to create new structures is that it allows us to probe the electronic properties of the new structure we create. For example, in Fig. 7C a spectroscopic current versus voltage measurement on the created 2-D Cs phase is displayed; this one-atomic layer of Cs atoms is insulating instead of exhibiting metallic conduction characteristic of bulk Cs (similar nonmetallic properties are found for the 1-D structures) (*10*).

The adsorption of CO on Pt(111) is one of the most thoroughly studied systems in modern surface science (*32*). CO is known to bind to the on-top and bridge sites of the Pt(111) surface and forms a variety of ordered overlayers according to conditions of temperature and coverage. In the $(\sqrt{3} \times \sqrt{3})$ R30° structure the CO binds to the on-top sites. We have imaged CO on the Pt(111) surface at 4 K in the low-coverage limit and found that CO may be repositioned on the Pt(111) surface with the sliding process (*17, 20*). We cannot determine the binding site of CO on the Pt(111) surface from STM images because junction resistances necessary to resolve the Pt(111) lattice are already well below the threshold resistance for manipulating CO on this surface. CO appears in one of two forms in our images (Fig. 6, B and C) (*33*). The appearance of a CO molecule may be changed between these two forms by sliding it to a new location on the surface. We refer to these forms as the "bump" and the "sombrero." Both are found to be stable over time, although the sombrero is somewhat delicate and readily converts to a bump (located just one half of one Pt nearest-neighbor distance away) if the tip is brought too close. We thus infer that the bump is the more energetically preferred state. We find that there is just one binding site per surface unit cell in which the CO appears as a bump, whereas there are multiple sites per surface unit cell in which the CO molecule can appear in the sombrero state. We have been able to assemble an island of bumps in the $(\sqrt{3} \times \sqrt{3})$R30° structure (Fig. 5A). Finally, we find [in contrast to the case of Xe on Ni(110)] that there is no range at which the adsorbate-adsorbate interaction appears to be attractive, that is, we see no evidence of bump-bump or sombrero-sombrero bonding. However, a sombrero may be stabilized against conversion to a bump if that sombrero is itself located adjacent to one or more bumps. All of this evidence is consistent with what we already know about CO on Pt(111) from other techniques, such as infrared spectroscopy, electron energy loss spectroscopy, and low-energy electron diffraction, if we assign the bump state to on-top CO and the sombrero state to bridge-bonded CO. In this way, we have used our manipulative abilities to help assign bonding sites to the different states in which CO appears on this surface (*34*).

The ability to manipulate matter with atomic-scale precision suggests that molecular synthesis is possible with the STM. There are several motivations for such synthesis. One could study how the environment of the reactants affects surface reactions, or how the conformation of reactants affects reaction barriers. Indeed, if one could successfully conduct such studies with an atomic force microscope (AFM) it would be possible to study the forces between reactants as a function of conformation. Manipulation combined with force measurement seems particularly useful. As an example, if one could measure the force on an atom during the sliding process, then it would be possible to map the potential between the atom and the surface. It should be possible to use the AFM to image and manipulate metal atoms on an insulating substrate, which would open the door to the study of electron transport in extremely small structures.

As we have discussed, the transfer-near-contact process is thermally activated. Since we may tune the height of the energy barrier by adjusting the position of the tip, conditions can be found such that the thermally activated hopping of the adsorbate occurs on an accessible time scale. By measuring the conductance of the tunnel junction it should be possible to monitor the hopping of the adsorbate (*21*). For each height of the tip above the sample we should be able to deduce the preexponent and the barrier height by measuring the temperature dependence of the hopping rate. We may thus map out the dependence of the barrier on the tip-surface separation.

In summary, we have discussed two classes of atomic manipulation processes with the STM and the mechanisms by which they are thought to work. Our understanding of certain mechanisms (for example, electromigration), and whether they constitute a correct explanation of the observed behavior, is clearly in its infancy. We anticipate that this situation will improve as an increasing body of data from different laboratories becomes available. These manipulation capabilities (which are also clearly in their infancy) are already being applied as a laboratory tools, and numerous applications are both fruitful and imminent.

REFERENCES AND NOTES

1. For a review of the STM, see P. K. Hansma and J. Tersoff, *J. Appl. Phys.* **61**, R1 (1987).
2. Two reviews of surface modification with the STM are in press: U. Staufer, in *Scanning Tunneling Microscopy II*, H.-J. Güntherodt and R. Wiesendanger, Eds. (Springer, Berlin, in press); and C. F. Quate, in *Proceedings of the NATO Science Forum '90*, L. Esaki, Ed. (Plenum, New York, in press).
3. R. P. Feynman, *Eng. Sci.* **1960**, 22 (February 1960).
4. E. W. Muller and T. T. Tsong, *Field Ion Microscopy* (American Elsevier, New York, 1969).
5. T. T. Tsong and G. Kellogg, *Phys. Rev. B* **12**, 1343 (1975).
6. S. C. Wang and T. T. Tsong, *ibid.* **26**, 6470 (1982).
7. E. V. Klimenko and A. G. Naumovets, *Sov. Phys. Solid State* **13**, 25 (1971); *ibid.* **15**, 2181 (1974).
8. L. J. Whitman, J. A. Stroscio, R. A. Dragoset, R. J. Celotta, *Science* **251**, 1206 (1991).
9. P. N. First, R. A. Dragoset, J. A. Stroscio, R. J. Celotta, *J. Vac. Sci. Technol. A* **7**, 2868 (1989).
10. L. J. Whitman, J. A. Stroscio, R. A. Dragoset, R. J. Celotta, *Phys. Rev. Lett.* **66**, 1338 (1991).
11. D. Heskett, N. J. DiNardo, E. W. Plummer, *J. Vac. Sci. Technol. B* **7**, 915 (1989).
12. J. Hebenstreit, M. Heinemann, M. Scheffler, *Phys. Rev. Lett.* **67**, 1031 (1991).
13. M. Krauss and W. J. Stevens, *J. Chem. Phys.* **93**, 8915 (1990).
14. The interaction between the adsorbate and the tip may have components due to the electric field and the tunnel current that under some circumstances could play an important role in the sliding process. The motion of Xe on Ni(110) in the sliding process that we have used is not sensitive to the sign or the magnitude of the electric field, the voltage, or the current. It is only dependent upon the separation of the tip from the adsorbate, from which we deduce that the bonding force is the dominant interaction between the adsorbate and the tip. We find similar results for sliding Pt adatoms and for adsorbed CO molecules (D. M. Eigler, unpublished results).
15. It is also possible to push atoms with the sliding process by simply bringing the tip close enough to the adsorbate so as to operate on the repulsive part of the adsorbate-tip interaction curve.
16. D. M. Eigler and E. K. Schweizer, *Nature* **344**, 524 (1990).
17. *New Sci.* **129**, 20 (23 February 1991).
18. P. F. Schewe, Ed., *Physics News in 1990* (American Institute of Physics, New York, 1990), p. 73 and cover.
19. D. M. Eigler, unpublished data.
20. P. Zeppenfeld, D. M. Eigler, C. P. Lutz, in preparation.
21. D. M. Eigler, C. P. Lutz, W. E. Rudge, *Nature* **352**, 600 (1991).
22. R. Gomer, *IBM J. Res. Dev.* **30**, 428 (1986).
23. T. T. Tsong, unpublished results.
24. R. S. Becker, J. A. Golovchenko, B. S. Swartzentruber, *Nature* **325**, 419 (1987).
25. H. J. Mamin, P. H. Guethner, D. Rugar, *Phys. Rev. Lett.* **65**, 2418 (1990).
26. D. W. Abraham, H. J. Mamin, E. Ganz, J. Clarke, *IBM J. Res. Dev.* **30**, 492 (1986).
27. D. Cleary, *New Sci.* **129**, 31 (26 January 1991).
28. Hitachi, Ltd., press release (14 January 1991).
29. I.-W. Lyo and P. Avouris, *Science* **253**, 173 (1991).
30. A. H. Verbruggen, *IBM J. Res. Dev.* **32**, 93 (1988).
31. K. S. Ralls, D. C. Ralph, R. A. Buhrman, *Phys. Rev. B* **40**, 11561 (1989).
32. Y. J. Chabal, *Surf. Sci. Rep.* **8**, 211 (1988), and references therein.
33. CO bonds to the Pt(111) surface with the C atom closest to the surface and the axis of the molecule normal to the surface. Therefore the molecule appears cylindrically symmetric in STM images.
34. The reader is left to ponder (as do we) what changes occur in the electronic structure that make bridge-bonded CO appear so different from on-top CO.

New Quantum Structures

MANI SUNDARAM, SCOTT A. CHALMERS, PETER F. HOPKINS, ARTHUR C. GOSSARD

Structures in which electrons are confined to move in two dimensions (quantum wells) have led to new physical discoveries and technological applications. Modification of these structures to confine the electrons to one dimension (quantum wires) or release them in the third dimension, are predicted to lead to new electrical and optical properties. This article discusses techniques to make quantum wires, and quantum wells of controlled size and shape, from compound semiconductor materials, and describes some of the properties of these structures.

THERE HAS BEEN SWIFT PROGRESS IN RECENT YEARS IN THE synthesis of artificial quantized structures. Electrons in these small structures show quantum effects that strongly modify their behavior. Progress has been especially rapid in layered quantum structures (*1*), which are stacks of precisely deposited thin films in which electrons show fundamentally new electrical and optical properties. These materials offer a miniature laboratory that has influenced our basic understanding of solids and has provided new kinds of optical and electronic devices (*2*). Among the discoveries emerging from layered structures are the quantum Hall effect (*3*) (for which the 1985 Nobel Prize in Physics was awarded), transistors with record speed, and lasers with record low threshold currents for lasing. Practical application of the structures has been so rapid that they are encountered now in our daily lives. Devices currently being manufactured with layered quantum structures include most lasers in compact disc players, low noise amplifiers in direct broadcast satellite receivers, and laser sources for fiber optic communication.

Past research on quantized semiconductor structures has focused on layered structures that confine conduction electrons to two dimensions. Now, systems in which the electrons are confined to one dimension of free motion (quantum wires) are providing materials with remarkable new properties [for instance, the quantization of electrical conductance in ballistic quantum wire channels (*4*)]. But the challenges of fabricating these wire-like structures are greater than those for making layered structures, and extensive improvements in the fabrication techniques are needed. A starting point for the fabrication of quantum wires has often been two-dimensional layered structures that are lithographically processed to achieve lateral confinement. But higher performance will require the fabrication of smaller structures for which it will probably be necessary to actually control the lateral motion of atoms during growth of the materials. This presents a major challenge in growth technology for the next generation of quantum structures.

The authors are in the Department of Electrical and Computer Engineering, and Materials Department of the University of California, Santa Barbara, CA 93106.